Evaluation of Virtual Observation Points for Local SAR Monitoring of Multi-Channel Transmit RF Coils at 7 Tesla

Andreas K Bitz[1], Rene Gumbrecht[2,3], Stephan Orzada[1], Hans-Peter Fautz[2], and Mark E Ladd[1,4]

[1]Erwin L. Hahn Institute for MRI, University of Duisburg-Essen, Essen, Germany, [2]Siemens Healthcare, Erlangen, Germany, [3]Department of Physics, Friedrich-Alexander University, Erlangen, Germany, [4]Department of Diagnostic and Interventional Radiology and Neuroradiology, University Hospital Essen, Essen, Germany

Introduction: With the application of multi-transmit approaches in high-field MRI, SAR monitoring becomes a challenging task, since several channels have to be supervised simultaneously and the local SAR has to be taken into account in addition to global SAR aspects. To accomplish this task for RF shimming systems, a procedure has been presented by Brote et al[1]. For the general case in which a different waveform is played out in every Tx channel, this concept is inapplicable due to the rather long computation time, which makes it impossible to calculate the resulting SAR in the time interval between two samples of the complex waveforms. To allow for online local SAR supervision, a more generalized approach has been published by Eichfelder and Gebhardt[2] and implemented on a parallel Tx 7T MRI system (TIM Tx Array Step 2, Siemens HealthCare). This approach is based on a local SAR model determined from numerical field simulations for the exposure scenario under investigation. From the numerical results a set of so-called local SAR matrices $S_n \in \mathbb{C}^{K\times K}$ (K = Tx channels) is calculated which include normalized information on the effect of the superimposed field distribution on the SAR in any volume n containing 10 g tissue mass (IEC standard 60601-2-33). Subsequently, virtual observation points (VOPs) are determined from the local SAR matrices by applying a lossy compression algorithm with a specified maximum SAR overestimation. It is not possible to calculate the exact local SAR from the compressed data, but an estimate with an unknown error which is in every case limited by the maximum overestimation. Hence, the predicted local SAR using the compressed data is always larger or equal to the predicted local SAR using the full model data. In the following, it is described how the simulation data can be properly transformed to calculate SAR matrices; furthermore, VOP models are evaluated for realistic exposure configurations with multi-channel Tx arrays.

Materials & Methods: Calculations are performed for two 7T RF coils, an 8-channel head coil and an 8-channel body coil, and for three different body models (male: 95 kg and 70 kg; female: 59 kg). The simulation models take into account the MR environment (bore, gradient shield, etc.) and the matching/tuning network including connecting cables to the coil plug at the patient table. The numerical models were previously validated[3]. Field distributions for the individual channels are calculated for a normalized RF excitation at the coil plug. After this, the complex vectors for the electric field components $\underline{E}_x(l)|_{i,j,k}$, $\underline{E}_y(l)|_{i,j,k}$, and $\underline{E}_z(l)|_{i,j,k}$ are set up in each mesh cell i, j, k containing the field produced by transmit channel l, with $l = 1, \dots, K$ (K = number of Tx channels). Afterwards, local SAR matrices are calculated in the mesh cells of the discretized body model by use of the electrical conductivity σ and tissue density ρ assigned to the cells: $\tilde{S}_{i,j,k} = \sigma_{i,j,k}/\rho_{i,j,k}\left(E_x|_{i,j,k}E_x{}^H|_{i,j,k} + E_y|_{i,j,k}E_y{}^H|_{i,j,k} + E_z|_{i,j,k}E_z{}^H|_{i,j,k}\right)$. A spatial averaging scheme (cubic averaging volume, interpolation to averaging mass of 10 g +/- 5%) is subsequently applied to obtain 10g-averaged local SAR matrices S_n to which the compression algorithm is applied to finally obtain the VOPs. Computational cost of the calculation is rather high, since SAR matrices S_n and $\tilde{S}_{i,j,k} \in \mathbb{C}^{8\times 8}$. Hence, a multi-threaded program code was developed. Validation of the generated VOPs was performed for each configuration on the MR scanner by comparing the maximum SAR_{10g} for selected excitation modes of the coil arrays, e.g. CP^+ or CP^{2+}, to the corresponding result obtained from the full data set, of course under consideration of the specified overestimation. Finally, the efficiency of the VOP compression was evaluated for the different coil and body configurations and for different SAR overestimation factors, as well as for combined models which include different locations including worst case positions in the head coil.

Results & Discussion: Validation of the VOP models was performed successfully for all configurations. Fig. 1 shows the results for the head coil and three body models, with the head centered and in a worst case position close to the lower coil element. Fig. 2 gives the results for the body coil and two body models. The number of human tissue mesh cells in the model, which is equal to the number of SAR matrices, varied for the different simulation models from 1 to 4 million. Decreasing the maximum overestimation increases the size of the compressed data set and, consequently, the calculation times during real-time monitoring on the scanner. For a reasonable maximum overestimation of 10%, the number of VOPs stayed below 500, for which online monitoring was tested successfully. It is expected that up to several thousand VOPs can be monitored online without exceeding critical calculation times on the scanner, which would result in abortion of the current scan. In practice, even an overestimation higher than 10% with corresponding fewer VOPs would be acceptable. The total number of VOPs occasionally depends strongly on the particular configuration. The higher the interference of the field patterns from the individual channels, the higher the number of VOPs. This applies, for example, to the female head for the centered position in the head coil (Fig. 1c). Compared to the larger heads of the male body models, for the female the distance to the individual coil elements is larger, resulting in broader field patterns and, thus, stronger interference. This effect is less pronounced for the body coil, which can be flexibly adjusted to the body contour. On the other hand, due to the female's smaller abdominal size, the field patterns of the channels can possibly show higher interference. Furthermore, the number of VOPs depends also on the efficiency of the implemented compression algorithm. The algorithm always finds a safe set of VOPs, but these do not necessarily represent the ideal solution for every configuration. This will be investigated further.

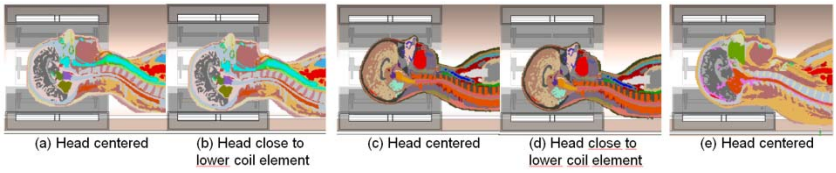

(a) Head centered (b) Head close to lower coil element (c) Head centered (d) Head close to lower coil element (e) Head centered

Body model (sex / weight)			(a) m / 70 kg	(b)	(c) f / 59 kg	(d)	(e) m / 95 kg
# VOPs	Over-estimation	1%	6783	-	-	-	-
		5%	260	357	747	326	131
		10%	60	88	164	69	29
			Combination (a)+(b)+(c)+(d)+(e)				
# VOPs	Over-estimation	5%	376				
		10%	70				

Figure 1: VOP evaluation for the 8-channel head coil and three body models

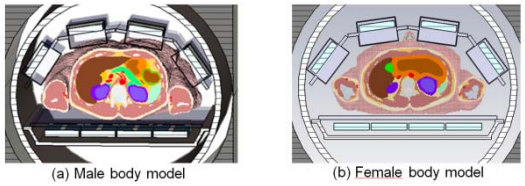

(a) Male body model (b) Female body model

Body model (sex / weight)			(a) m / 70 kg	(b) f / 59 kg
# VOPs	Over-estimation	5%	322	450
		10%	80	109
			Combination (a)+(b)	
# VOPs	Over-estimation	5%	650	
		10%	148	

Figure 2: VOP evaluation for the 8-channel body coil

Conclusion: The VOP approach considerably reduces the complexity of SAR calculation for arbitrary excitation of multi-channel Tx arrays and, thereby, enables online SAR monitoring for multi-dimensional RF pulses. Additionally, it is possible to combine configurations with various body positions with respect to the RF coil and/or various body sizes in a single VOP data set. Thus, generalized VOP models can be used to monitor a broader range of exposure scenarios with a single data set.

References: [1] Brote I et al. ISMRM Safety Workshop 2010. [2] Eichfelder and Gebhardt, MRM 66:1468-1476 (2011). [3] Bitz AK et al. Proc. ISMRM 19 (2011), 490.